

## Journal Pre-proof

Spontaneous back-pain alters randomness in functional connections in large scale brain networks: A random matrix perspective

Gurpreet S. Matharoo, Javeria A. Hashmi

PII: S0378-4371(19)31860-6  
DOI: <https://doi.org/10.1016/j.physa.2019.123321>  
Reference: PHYSA 123321

To appear in: *Physica A*

Received date: 22 April 2019  
Revised date: 5 October 2019

Please cite this article as: G.S. Matharoo and J.A. Hashmi, Spontaneous back-pain alters randomness in functional connections in large scale brain networks: A random matrix perspective, *Physica A* (2019), doi: <https://doi.org/10.1016/j.physa.2019.123321>.

This is a PDF file of an article that has undergone enhancements after acceptance, such as the addition of a cover page and metadata, and formatting for readability, but it is not yet the definitive version of record. This version will undergo additional copyediting, typesetting and review before it is published in its final form, but we are providing this version to give early visibility of the article. Please note that, during the production process, errors may be discovered which could affect the content, and all legal disclaimers that apply to the journal pertain.

© 2019 Published by Elsevier B.V.



# Spontaneous back-pain alters randomness in functional connections in large scale brain networks: A random matrix perspective

Gurpreet S. Matharoo<sup>1,2\*</sup> and Javeria A. Hashmi<sup>3†</sup>

<sup>1</sup> ACENET, St. Francis Xavier University, Antigonish, NS, B2G 2W5, Canada.

<sup>2</sup> Department of Physics, St. Francis Xavier University, Antigonish, NS, B2G 2W5, Canada.

<sup>3</sup> Department of Anesthesia, Pain Management and Perioperative Medicine, Dalhousie University, Halifax, NS, Canada.

\* [gmatharo@stfx.ca](mailto:gmatharo@stfx.ca) (Corresponding author)

† [javeria.hashmi@dal.ca](mailto:javeria.hashmi@dal.ca)

## Highlights:

- Brain networks impacted by back-pain are analyzed from random matrix theory perspective.
- The study demonstrates the effectiveness of random matrix theory in differentiating between resting state and two distinct task states within the same patient.
- Random matrix theory is effective in measuring systematic changes occurring in functional connectivity.
- This study offers new insights on how acute and chronic pain are processed in the brain at a network level.

## Abstract

We use randomness as a measure to assess the impact of evoked pain on brain networks. Randomness is defined here as the intrinsic correlations that exist between different brain regions when the brain is in a task-free state. We use fMRI data of three brain states in a set of back pain patients monitored over a period of 6 months. We find that randomness in the task-free state closely follows the predictions of Gaussian orthogonal ensemble of random matrices. However, the randomness decreases when the brain is engaged in attending to painful inputs in patients suffering with early stages of back pain. A persistence of this pattern is observed in the patients that develop chronic back pain, while the patients who recover from pain after six months, the randomness no longer varies with the pain task. The study demonstrates the effectiveness of random matrix theory in differentiating between resting state and two distinct task states within the same patient. Further, it demonstrates that random matrix theory is effective in measuring systematic changes occurring in functional connectivity and offers new insights on how acute and chronic pain are processed in the brain at a network level.

**Key Words:** Random Matrix Theory, Back-pain, Functional MRI, Brain Networks

## 1. Introduction

Chronic pain represents a major clinical, social, and economic problem for societies worldwide. The principal complaint is of unremitting physical pain that does not abate with standard analgesics [1–3]. The experience of pain is quite different across the population and persists for different durations between individuals. Pain is in essence a threat signal that we localize to a part of the body in the form of an unpleasant sensation. This sensation accompanies a strong negative emotion that works as an aversive signal which is necessary for learning proper avoidance behaviors. In some people, this signal becomes accentuated and tends to persist for long periods of times extending over months to years. These individuals very often show no signs of tissue damage or underlying pathology in the site where they are feeling pain. Brain imaging studies suggest that chronic pain alters the nervous system so that the brain perceives persistent pain due to maladaptive processes in the brain. An expedient approach for understanding these maladaptive processes is to observe how back pain transitions to a chronic form.

Thus, we know that in some patients, persistent back pain is acute and persists for a few weeks to be classified as subacute back pain (or SBP). This early stage of persistent back pain remits in some individuals, while for others, it persists for months to years and this enduring back pain is classified as chronic (Chronic Back Pain or CBP). Brain responses to back pain have been reported to change over time as people with subacute back pain develop chronic back pain. While any initial instance of self-report of spontaneous occurrence of back pain activates brain regions such as the insula and the anterior cingulate cortex that customarily respond to acutely evoked pain, over time, these instances correspond with activations in regions that process fear (amygdala) and self-referential thinking (medial prefrontal cortex). In a recent longitudinal study [3], it has been clearly demonstrated (with pictorial representations) that persistence of back pain alters brain responses. A large cohort of people with CBP, it was established that brain connectivity is also altered by persistent pain, where regions with the highest connectivity (hubs) show a deviation in their pattern across the brain relative to healthy controls and shows increases in modularity in sensory areas of the brain [4].

The reasons and neural mechanisms due to which back pain transitions from subacute to chronic are still ambiguous, and the pursuit to find neurological reasons for this transition is central to contemporary pain research. In recent years, there have been successful attempts in relating CBP to specific brain activity [5] whereby neuroimaging method of functional Magnetic Resonance Imaging (fMRI) is used to study the correlations between CBP and brain activity. fMRI makes use of the fact that neuronal activity is partly coupled with increases in blood flow in the observed parts of the brain and it images these changes as a haemodynamic response to brain activity. This particular form of fMRI is also referred to as blood-oxygenation-level-dependent (BOLD) fMRI and it offers high spatial resolution. A useful adaptation of this approach is to measure how slow temporal fluctuations (0.01-0.15 HZ) are between different brain regions and this statistical dependency is referred to, more generally, as functional connectivity. Identification of functional networks from fMRI data has gained importance in the recent years as it provides critical information about correlations between different regions of brain, and how these correlations are affected in various conditions [6,7]. The network properties that emerge from large-scale correlations have been shown to be altered in neuropsychiatric and chronic conditions such as CBP[5,8–12]. It is still a challenge to understand the dynamic transition of brain between different

93 states as a result of back-pain. It is because brain is a fairly complex system whereby neurons are  
94 constantly interacting with each other often resulting in higher brain functions [13,14] and in the  
95 formation of functional networks, even in the absence of any stimuli. Though large-scale  
96 functional connectivity is often studied using clustering techniques or principles of graph  
97 theory[15], there is a need to apply the concepts and methodologies developed in the context of  
98 the theory of random matrices for observing systematic transitions in brain states.

99  
100 Random Matrix Theory (RMT) was originally developed in the nuclear physics applications,  
101 where nuclei can have many possible states and energy levels and, and their interactions are too  
102 complex to be described accurately. In such a scenario, one settles for a model that captures the  
103 statistical properties of the energy spectrum. RMT finds extensive applications in the statistical  
104 studies of various complex systems such as quantum chaotic systems, complex nuclei, atoms,  
105 molecules, disordered mesoscopic systems [16–24], atmosphere [25], financial applications [26],  
106 complex networks [27], societal networks [28], network forming systems [29,30], amorphous  
107 clusters [31–34], biological networks [35], protein networks [36,37], and cancer networks [38]  
108 etc. In recent years, RMT has also been applied towards brain network studies in studying universal  
109 behavior of brain functional connectivity and has been effective in detecting the differences in  
110 resting state and visual stimulation state[39,40]. Recently, attempts using RMT have also been  
111 made in brain functional network studies on attention deficit hyperactivity disorder (ADHD) [41].

112  
113 RMT makes use of the fact that true information of the system is contained in the eigenvalues of  
114 a correlation matrix. Specifically, for brain networks, the eigenvalues represent the level of  
115 functional connectivity between different regions of interest (ROIs) in brain, and larger  
116 eigenvalues contain information about significant correlations (or strong connectivity), and  
117 therefore, about processes in brain. Recent studies have shown that ROIs in brain are correlated.  
118 Furthermore, these correlations closely follow the predictions of Gaussian Orthogonal Ensemble  
119 (GOE) of random matrices when the brain is in a state of rest (fully conscious). The clearest  
120 indication so far has come from EEG data[39], which further attributes the observed deviation  
121 from GOE predictions to visual stimulation; that is, true information. Other recent studies[40,41]  
122 also point to similar information, however, the overall findings are unclear. We hereby propose a  
123 hypothesis where, we refer to these observed correlations as random correlations, or in general,  
124 randomness, that exists at any given instant in brain network. When the brain is engaged in a task,  
125 this randomness would be expected to decrease, as brain regions would be connected in a coherent  
126 fashion relative to a task-free or resting state. These random correlations reach their normal levels  
127 at resting state. Thus, RMT may offer a principled approach for measuring systematic changes in  
128 randomness that occur in brain networks during perception and cognition.

129  
130 Here we investigate whether the brain demonstrates a greater deviation from GOE predictions  
131 when it is engaged in detecting threats or experiencing discomfort from pain relative to perception  
132 of innocuous stimuli. Since the ability to properly detect and perceive pain is fundamental for  
133 survival, attending to pain can be expected to add systematic changes in brain connectivity and  
134 thus reduce random correlations in brain networks. On the other hand, maladaptive processing of  
135 pain inputs during a chronic stage of back pain may show a different behavior, relative to the SBP  
136 state. The ability to distinguish these two states using an integrative approach such as RMT could  
137 be useful for improving chronic pain diagnosis and prognosis and also for understanding the  
138 abnormalities in brain properties that contribute to CBP.

139

140

## 2. Materials and methods

141

142 In the following sub-sections, we describe the methodology and the workflow that we have  
143 followed for the present work in a chronological order:

144

### 2.1 Subject Classification

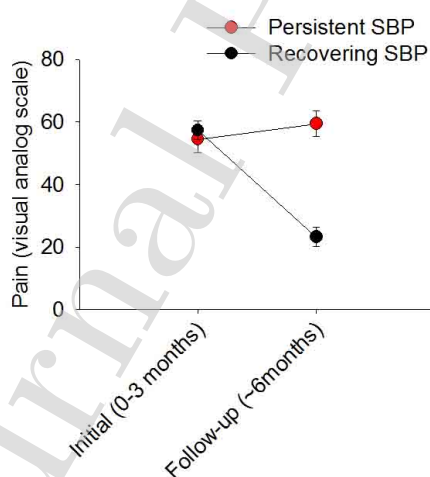
145

146 For the present work, we use fMRI data available on the open access data sharing platform for  
147 brain imaging studies of human pain (www.openpain.org). The complete dataset is a part of 5-year  
148 longitudinal study of transition to chronic back pain in which 120 patients were recruited initially.  
149 At each visit, fMRI scans and McGill Pain Questionnaire Visual Analogue Scale (MPQVAS)  
150 measures were recorded for all the patients.  
151

152

153 For the present RMT-based study, we use fMRI scans obtained from two visits namely, an initial  
154 visit where all patients report back-pain, and a follow-up visit six months after the initial visit,  
155 whereby some patients report remission of back-pain and others report persistence of back-pain.  
156 As a result, at the follow-up visit, based on the difference of MPQVAS measures for the two visits,  
157 the patients are classified in two groups. For group of patients whose MPQVAS values decrease  
158 by 30% or more than the corresponding value at initial visit, we classify them as “SBP recovering  
159 (or simply, recovering)” group, and the rest as “SBP persistent (or simply, persistent)” group. A  
160 pictorial representation of this classification is illustrated in Figure 1.  
161

161



162 **Fig. 1:** Recovering SBP group in contrast to Persistent SBP group based on MPQVAS ratings.  
163 Each of the points denotes the mean value for the group. The error bars represent standard error of  
164 mean.

165

166

167

168

### 2.2 fMRI Tasks

169  
170 All the participants were trained to perform two tasks using finger-span device with which they  
171 provided continuous pain ratings[3,5]. This device consisted of a potentiometer in which voltage  
172 was digitized. During the brain imaging sessions, the device was synchronized and time-stamped  
173 with fMRI image acquisition and connected to a computer providing visual feedback of the pain  
174 ratings [42]. We use data acquired from three different states:

175  
176 **a) Resting State (RS):** A state of rest in which the participants are not thinking about any one  
177 thing in particular.

178  
179 **b) Spontaneous Pain (SP):** A state of focusing and rating spontaneous changes in back pain.  
180 Here, the individuals saw a bar that increased or decreased in height on the y-axis scale (0-100).  
181 By changing the distance between the thumb and index finger, they could increase or decrease the  
182 height based on the intensity of pain they felt in their back on the scale. These measurements were  
183 recorded in real time and individuals continuously rated their back pain during the length of the  
184 entire brain scan.

185  
186 **c) Standard Visual (SV):** A control state in which they are rating changes in length of a visual  
187 bar. Here, participants no longer rated their pain, instead they increased or decreased the distance  
188 between their fingers so that it matched the changes in the height of the bar on the scales y-axis.  
189 Thus, the SV condition represents a control condition that was unrelated to pain and only represents  
190 a visual-motor control task.

### 191 192 **2.3 MRI data acquisition**

193  
194 The data for all participants and visits was collected by a 3T Siemens scanner. At first, MPRAGE  
195 type T<sub>1</sub> anatomical brain images were acquired followed by fMRI scans on the same day with the  
196 following parameter details [3]: EPI sequence: voxel size 1 X 1 x1 MM, Repetition time=2500MS;  
197 Echo Time=3.36MS; Flip angle = 9 degrees; In-Plane matrix resolution 256 X 256; slices 160,  
198 filed of view, 256mm. Functional MRI scans were acquired on the same day as the T1 scan and  
199 McGill Pain Questionnaire Visual Analogue Scale (MPQVAS) measures: multi-slice T2\*-  
200 weighted EPI images with repetition time=2.5s, echo time=30ms, flip angle =90 degree, number  
201 of volumes =244, slice thickness =3mm, in-plane resolution =64 x 64.

### 202 203 **2.4 Pre-processing of fMRI data**

204  
205 We use Freesurfer, FMRIB Software Library (FSL) v5.0, and Analysis of Functional Neuro-  
206 Images (AFNI) software to preprocess the data similar to procedures adapted for the 1000  
207 Functional Connectomes project[43]. Data were slice time corrected, motion corrected, temporally  
208 band-pass filtered, and then further filtered to remove linear and quadratic trends using AFNI.  
209 Complete details of the preprocessing procedure are given in[44]. The registration was performed  
210 using FMRIB's Linear and non LINEAR Image Registration Tools for transformations from native  
211 functional and structural space to the Montreal Neurological Institute MNI152 template with 2 x  
212 2 x 2 resolution, with further details given in[44].

### 213 214 **2.5 Anatomical parcellation and construction of correlation matrix**

215  
 216 The brain is anatomically parcellated by *an optimization of the Harvard/Oxford parcellation*  
 217 *scheme* (OHOPS)[45]. In this scheme, the anatomical partitioning of cingulate, medial and lateral  
 218 prefrontal cortices of Harvard Oxford Atlas was increased and in addition, anatomical partitioning  
 219 of insular label was also performed, and the single Region of Interest (ROI) spanning the entire  
 220 insula in Harvard Oxford Atlas was further subdivided based on a previous scheme[46]. The  
 221 complete OHOPS consisted of a total of 131 regions[45]. Each ROI was designated as a node and  
 222 the BOLD time series were extracted from each node and averaged to generate 131 time series for  
 223 each subject. Following this, the whole brain networks were constructed, and network measures  
 224 were assessed using the Brain Connectivity Toolbox, with formulae used for calculating network  
 225 measures described in[47]. The brain networks are usually assortative in nature[48,49].  
 226

227 For each patient, the BOLD time series in each region was correlated with every other region to  
 228 create a 131 x 131 symmetric correlation matrix based on Pearson's correlation coefficients given  
 229 by:  
 230

$$231 \quad \text{corr}(X, Y) = \frac{\text{cov}(X, Y)}{\sigma_X \sigma_Y}$$

232  
 233 or, which can also be written as:  
 234

$$235 \quad \text{corr}(X, Y) = \frac{\sum_{i=1}^n (x_i - \bar{x})(y_i - \bar{y})}{(n-1) \sqrt{\frac{\sum_{i=1}^n x_i^2 - n\bar{x}^2}{n-1}} \sqrt{\frac{\sum_{i=1}^n y_i^2 - n\bar{y}^2}{n-1}}}$$

236  
 237 Here, X and Y are two distinct time series, each made up of  $n$  time points,  $x_i$  and  $y_i$  respectively.  
 238 For the present case, there are 240 time points ( $n = 240$ ) for each time series.  $\bar{x}$  and  $\bar{y}$  are the  
 239 respective means for two time series ( $x$  and  $y$ ). By definition, the diagonal elements of the matrix  
 240 are 1, as it represents self-correlation and the off-diagonal elements result in a symmetric matrix.  
 241 Such correlation matrices are not only symmetric, but they are also positive semi-definite[50,51],  
 242 with all eigenvalues being non-negative. This correlation matrix is then diagonalized and  
 243 eigenvalues ( $\lambda$ ) are obtained. In the present case, there are 131 eigenvalues, few eigenvalues are  
 244 zeros, and remaining have positive values. It must be remembered that not all ROIs are a part of  
 245 active brain network at a given time and hence, very small eigenvalues are usually ignored, and  
 246 the related correlations are unimportant from functional connectivity perspective. In the present  
 247 cases, usually the first 40 (around 30%) eigenvalues are extremely small from computational  
 248 perspective. Hence, we leave them out from the subsequent analysis.  
 249

## 250 **2.6 Unfolding of data**

251  
 252 Fluctuations around the eigenvalue spectra are studied using standard methods of RMT. The first  
 253 step is to unfold the data, meaning, the eigenvalues are arranged in an increasing (cumulative)  
 254 order and are then mapped using an analytical function in such a way that the average spacing  
 255 between two successive eigenvalues is unity. This ensures all the eigenvalues are on same footing.  
 256 The analytical fitting function used for unfolding need not be unique and, is generally different for

257 different systems[30–34]. For this study, the eigenvalue spectra of all the correlation matrices  
 258 generated is approximated extremely well by a function of the form

259

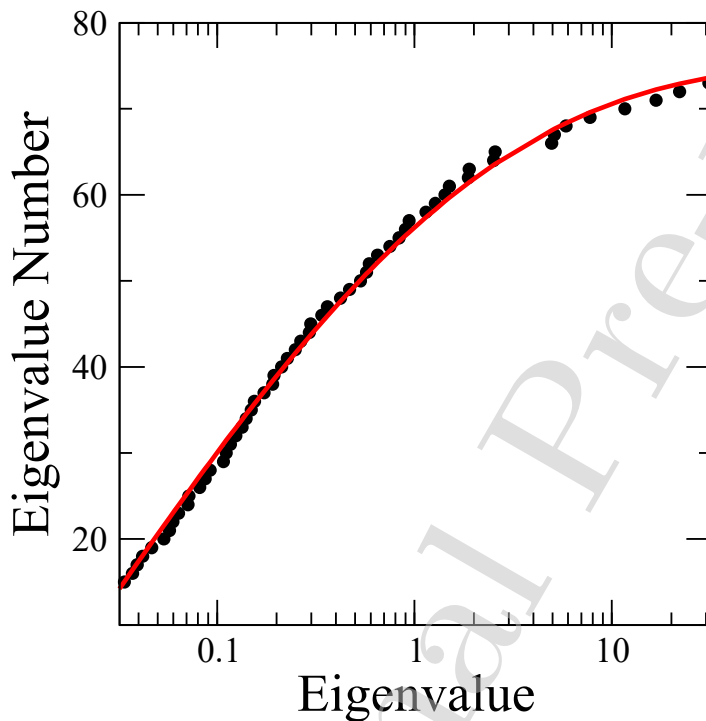
260

$$(a - b * e^{-c\lambda^{1/d}})$$

261

262 where a, b, c, and d, are best-fit parameters and  $\lambda$  is the eigenvalue. Figure 2 shows a plot of the  
 263 cumulative eigenvalue density along with the analytical fitting function. We leave out a small  
 264 portion of eigenvalues at the upper end (3 or 4 eigenvalues) in order to achieve the best fit,  
 265 something which has been a standard practice in other works [30–34]. We deal with unfolded  
 266 eigenvalues from this point onwards.

267



268

269

**Fig. 2:** Eigenvalue number vs eigenvalue ( $\lambda$ ) for a typical spectrum. Filled circles (black): Data.  
 270 Continuous line (red): The best-fit using the functional form described in text.

271

272

### 3. RESULTS

273

274 We report the spectral statistics fluctuation properties of the eigenvalue spectra in the three brain  
 275 states in individuals who were suffering with SBP (back pain for < 3 months). We also track what  
 276 these properties looked like after 6 months in the group of individuals with SBP with persisting  
 277 back pain[3,5,10,52]. Patients had all been pain free for one year prior to their subacute pain  
 278 episode and had no history of any mental illness including depression. The individual details of  
 279 patients are also available online on the data sharing platform. It must also be stated that none of  
 280 the data from available subjects was excluded from the analysis.

281



### 3.1 INITIAL VISIT

For the initial visit, where all patients report back-pain, 68 SP and 62 SV scans are available. In addition, there are 27 RS scans available. Analysis of randomly picked individual eigenvalue spectra indicate that brain-states have fluctuation properties associated with the Gaussian orthogonal ensemble (GOE) of random matrices. To improve statistics, we combine information from all unfolded data. Figure 3a shows the normalized nearest-neighbor spacing distribution (NNSD)  $[p(s)]$  for RS, SP, and SV scans for the initial visit. Here,  $s$  is the eigenvalue spacing. Superimposed is the GOE result, which is also approximated by Wigner's surmise as:

$$p(s) = \left(\frac{\pi s}{2}\right) * e^{-\pi s^2/4}$$

For all the cases, we find a good agreement with GOE. For RS scans, this is not really surprising. Here, the patients have been directed to remain awake and not to think on any one thing in particular. In such a scenario, we would expect maximum randomness, hence NNSD would agree with GOE. The agreement of SP and SV scans with GOE is however, a more interesting case. In SP scans, as the patients are focusing on their back-pain and simultaneously reporting the pain rating through the finger device, a lot of brain regions are expected to be involved in this task. As a result, if there were to be a deviation from the GOE, we would expect it to be in SP scans. However, we do not see any deviation of NNSD from the GOE results. Lastly, SV being a visual task, is an intermediate of RS and SP states. Here, patients are following a displayed visual while performing the finger-spanning task without specifically focusing on the back-pain, and once again, we find an excellent fit of NNSD with the GOE. A single-valued indicator that follows the  $p(s)$  function is the variance of nearest-neighbor spacing. We find this number between 0.297 and 0.320 for all the cases, which is quite close to 0.286, the number for GOE[31–33]. This agreement could be explained due to the fact that NNSD captures the correlations that exists between successive eigenvalues and does not have information about the long-range correlations. Short-ranged correlations, especially between the nearest-neighbors are quite strong, and hence not altered substantially by both, visual (SV) and pain-rating (SP) tasks. This result is also consistent to other brain-network studies[39–41,49] and hence, further strengthens the belief that there exists strong, stimuli-resistant random correlations between nearest-neighbors in the brain network.

Next, we take a look at the long-range (or higher order) random correlations. For this, we measure  $\Sigma^2(r)$ , the variance of the number of levels  $n(r)$  within an interval of length  $r$ . The theoretical result for GOE is:

$$\Sigma^2(r) = \frac{2}{\pi^2} \left( \ln(2\pi r) + 1.5772 - \frac{\pi^2}{8} \right)$$

The number variance is quite sensitive to changes, and is extremely sensitive to small systematic errors in the approximation to the analytical function used during unfolding[31,32]. Contribution of any such error to  $\Sigma^2(r)$  grows as  $r^2$ , whereas the GOE prediction for  $\Sigma^2(r)$  grows as  $\ln(r)$ [34]. In Figure 3b, we plot  $\Sigma^2(r)$  for RS, SP, and SV scans along with GOE and Poisson [ $\Sigma^2(r) = r$ ] distributions for the initial visit. We observe that RS agrees with the GOE prediction over greatest domain, whereas we do see deviations for SV and SP scans with SP scans showing maximum deviation. This deviation is attributed to the relative tasks the subjects are performing in each case,

326 with the pain-rating task showing maximum deviation. While it is on the expected lines to observe  
327 the variance agreement for RS scans to the GOE, it further demonstrates the efficacy of the RMT  
328 of capturing strong random long-ranged correlations when the brain is in a state of rest. We see a  
329 clear deviation from GOE for SP scans, whereby the patients are performing a pain-rating task. As  
330 stated before, a lot of brain regions are expected to participate in this task and, as a result, we see  
331 a clear decrease in randomness for SP scans. SV scans, however, present an interesting picture.  
332 We observe SV scans to show a good agreement with GOE for a greater range than SP scans,  
333 whereby the agreement matches with RS scans. While we do observe deviations from GOE  
334 eventually, the deviations are always less than SP deviations. This could be explained due to the  
335 nature of the task performed for SV scans. As the patients are not focusing on back-pain, the task  
336 involves only visual cortex to take part. In other words, compared to SP, this is an easier task to  
337 perform and, the difference between SV state and RS is quite subtle. As a result, fewer brain  
338 regions are expected to participate here. This inference is also consistent with the earlier results,  
339 whereby it is shown that salient percepts like pain engage more brain regions than visual  
340 stimulation[53–55]. This observed difference between the SP and SV scans is also the impact that  
341 SBP has on the brain networks. Additionally, also important here is the fact that RMT is able to  
342 capture the differences between two distinct task states.

### 343 3.2 FOLLOW-UP VISIT

344 At follow-up visit, which was approximately 6 months after the initial visit, the patients were made  
345 to repeat the same tasks (RS, SP and SV) and the corresponding scans were recorded. At this  
346 follow-up visit, while some patients recovered from persistent back-pain as a result of spontaneous  
347 remission of the condition (SBP recovering group), others experienced a persistence in their back-  
348 pain, and they represent the group who have developed chronic back-pain (persistent group). To  
349 define SBP persistent group, we separate participants with pain persisting for 6 months from those  
350 that recovered (SBP recovering) based on self-report of pain ratings observed using McGill Pain  
351 Questionnaire Visual Analogue Scale (MPQVAS). We compare the MPQVAS values at initial  
352 and follow-up visits. If the pain rating value of a particular subject decreases by 30% or more, the  
353 subject is classified as "Recovering", else, it is classified as "Persistent" (See Figure 1). Based  
354 on this classification, we have 18 RS, 17 SP, and 23 SV scans for Persistent group and 18 RS, 19  
355 SP, and 17 SV scans for Recovering group.

356 Figure 4 shows NNSD for Persistent and Recovering groups. In both the plots, we observe the  
357 same trend for NNSD as it was at the initial visit. In both the plots, all the scans show an agreement  
358 with GOE predictions; an indicator of strong nearest-neighbor random correlations. The tasks at  
359 the follow-up visit are exactly same as the initial visit's tasks. As a result, we can state with a  
360 greater certainty that the NNSD captures short-ranged correlations effectively, and the randomness  
361 is undeterred by the pain stimuli.

362 We now take a look at the long-ranged random correlations. As mentioned before, this quantity is  
363 quite sensitive to the network changes that occur over a period of time. Figure 5 shows plots of  
364  $\Sigma^2(r)$  for Persistent and Recovering groups. In both the cases, we find RS scans staying close to  
365 GOE predictions. This once again is on expected lines. However, we find a striking difference  
366 between SP and SV scans in the two cases.

371

372 For the Persistent group, both SP and SV scans show deviations from the theory, with SP scans  
373 clearly showing greater deviations from theory, and SV scans showing only subtle deviations. The  
374 clear deviations of SP scans from GOE for the persistent group is also a reflection of the fact that  
375 they continue to experience the back-pain, hence, they are prone to chronic back-pain. And, as in  
376 the case of initial visit, the subtle differences between SV scans and theory could once again be  
377 attributed to the fact that visual stimulation task involves engagement of fewer brain regions. The  
378 recovering group, however, present a very interesting case. For the Recovering group, both SP and  
379 SV scans match GOE predictions over a larger domain and are indistinguishable from RS scans.  
380 Here, as a result of the medical treatment, the patients have experienced pain remission. As a result,  
381 they have none to very few pain events to report for SP scans. This observation once again  
382 demonstrates the efficacy of RMT in capturing the network changes in brain networks.

#### 383 384 **4. Conclusions and Discussion**

385  
386 Randomness is inherent in all brain networks and it follows the characteristics of GOE of random  
387 matrices. The resting state can be assumed as a normal state, and it defines normal or equilibrium  
388 levels of randomness. Both, cognitive tasks and salient percepts (for example, pain) decrease  
389 randomness as they require more brain regions to be focused. In network concept, resting state  
390 could also be assumed as more random state or a disordered state [27], and cognitive tasks and  
391 salient percepts force it to be more ordered. Hence, task-states can also be interpreted as more  
392 ordered than the normal state. Mathematically, it means deviations from the GOE predictions.  
393 Once the tasks are over, or the salient percepts are no longer there, we would expect the  
394 randomness to reach its normal or equilibrium levels.

395  
396 For all the cases, our results demonstrate that the randomness shows maximum agreement with  
397 GOE for the RS scans and it decreases the most for SP scans. So, RS can be viewed as a most  
398 random state, and SP state can be viewed as a most-ordered state. SV state falls between the two.  
399 The resting state is important with regard to BOLD fMRI correlations, and the agreement with  
400 GOE could also be visualized as a single correlation structure that may adequately describe it [7].  
401 Also, the continued agreement of the RS scans with GOE is also consistent with the reasoning that  
402 resting state BOLD correlations reflect processes concerned with long term stability of brain's  
403 functional organization, and generally do not reflect short term changes in cognitive content [7].

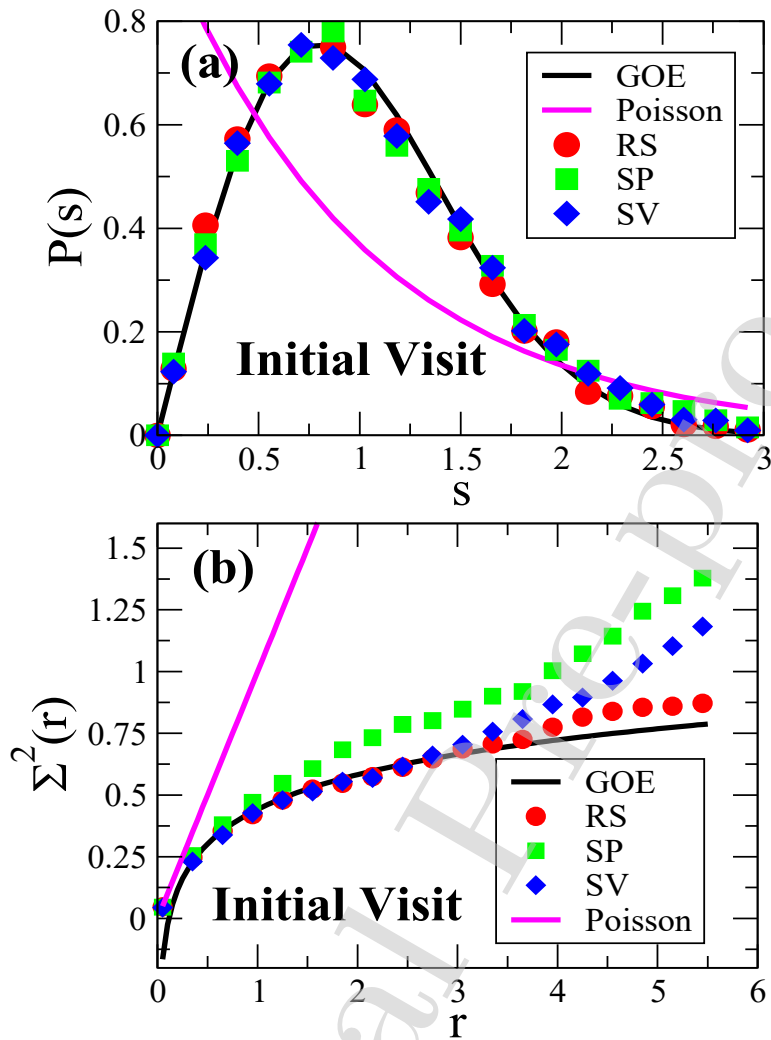
404  
405 Further, our results demonstrate that RMT is able to differentiate between two different tasks  
406 within the same subject. Here, we find a pattern consistent with our hypothesis, with randomness  
407 decreasing when the brain is focused on attending to pain triggered in the back of their body. Here,  
408 GOE line represents maximum randomness and Poisson represents no randomness. However, due  
409 to the complexity of the experimental design, there could be many possible conjectures (including  
410 their combinations) explaining these observations.

411  
412 First, as the patients are performing a pain-rating task, whereby they are focusing on the back-pain  
413 and reporting the ratings, the observed SP deviations could be attributed to back-pain. As it known  
414 from earlier studies that salient percepts such as pain are known to require more brain areas to be  
415 engaged than visual stimulation[53–55], we see an increased deviation for SP scans relative to SV  
416 scans in all the cases. As more brain regions are engaged in attending to pain, hence relative  
417 randomness between them decreases. At initial visit, all patients report back-pain, whereas at

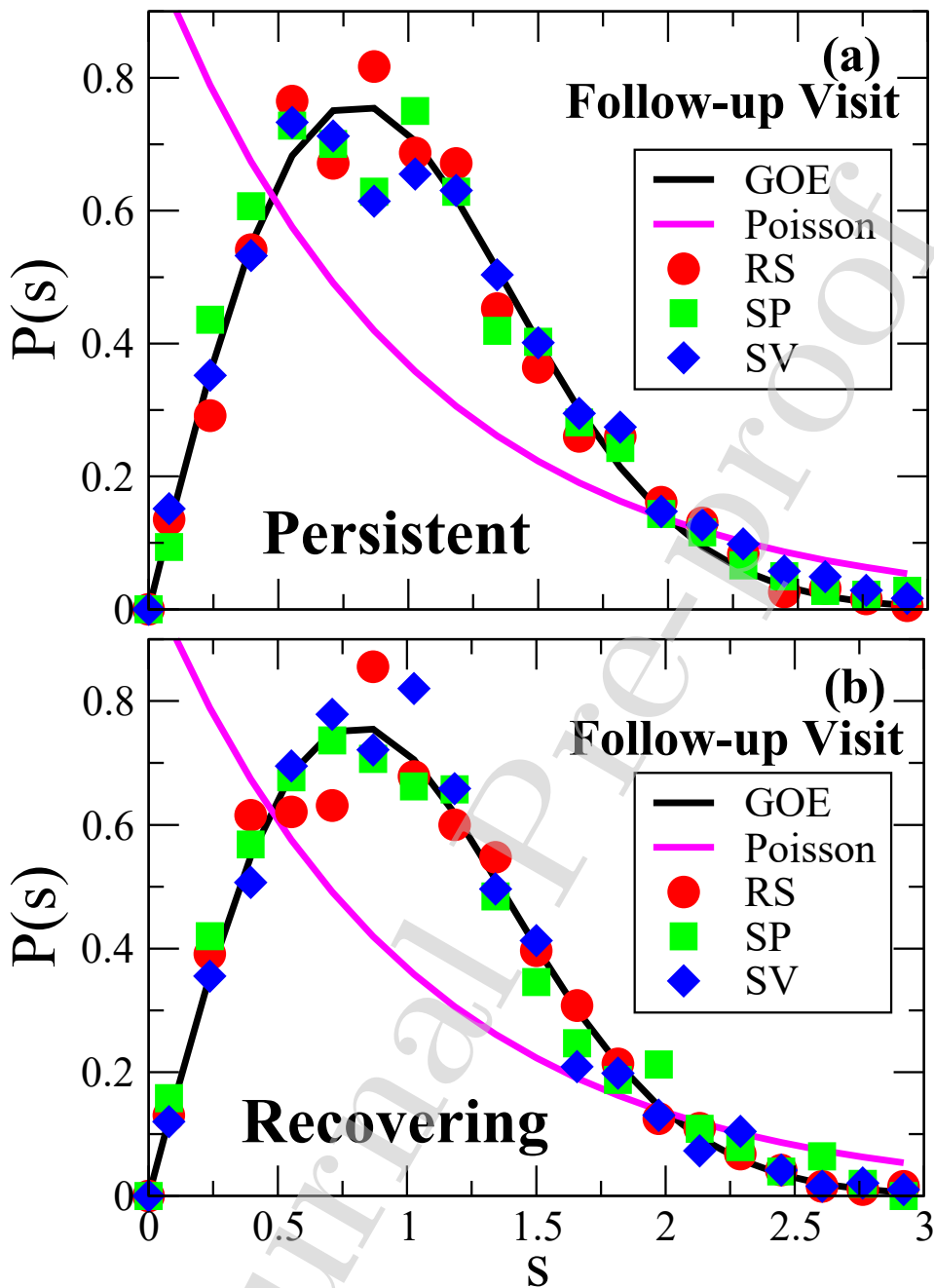
418 follow-up visit, only a subset of them report back-pain, and because their MPQVAS ratings  
419 demonstrate chronification of pain, the persistent group continues to experience back-pain over  
420 many months. Hence, this continued deviation of SP scans at the follow-up visit in the persisting  
421 CBP group could be viewed as a reflection of chronified pain that continues to affect the GOE  
422 pattern. It is also known that task states can alter the correlation structure of BOLD activity [7]  
423 and hence, the second possible conjecture is the saliency between the tasks themselves. While  
424 visual tasks are relatively easy to perform, pain-rating tasks could be much difficult as back-pain  
425 events are generally random. Hence, more attention is needed to perform these tasks, and thereby,  
426 we observe a decrease in randomness between the brain regions involved in these tasks.

427  
428 Finally, in spite of the complexities in the experimental design in the present work, the  
429 observations presented here prepare a platform to study fMRI generated brain-networks using  
430 RMT. RMT could be effectively used in studying metastability of brain networks impacted by  
431 other neuro-psychiatric disorders. Clues from RMT studies on other physical systems, especially  
432 liquids and amorphous solids, could be useful here. For example, normal modes studies on liquids  
433 [29,30] and amorphous systems [27–30] have revealed universal properties whereby, the  
434 fluctuations around the mean spectral densities for stable configurations (local minima) follow  
435 GOE, and deviations from GOE are observed for non-stable configurations. In this context, RMT  
436 could be used in the energy landscape studies of brain in the detection of metastable states. An  
437 inherent shortcoming of this method is that it is statistical in nature. However, suitable  
438 modifications and adaptations of the methodology in artificial neural networks would be extremely  
439 helpful. The fact that the resting state is a state with maximum randomness could then be used as  
440 a key component in determining any systematic or mechanical errors in fMRI scans. Also, it could  
441 reflect on the long-term stability of brain's functional organization.

442  
443

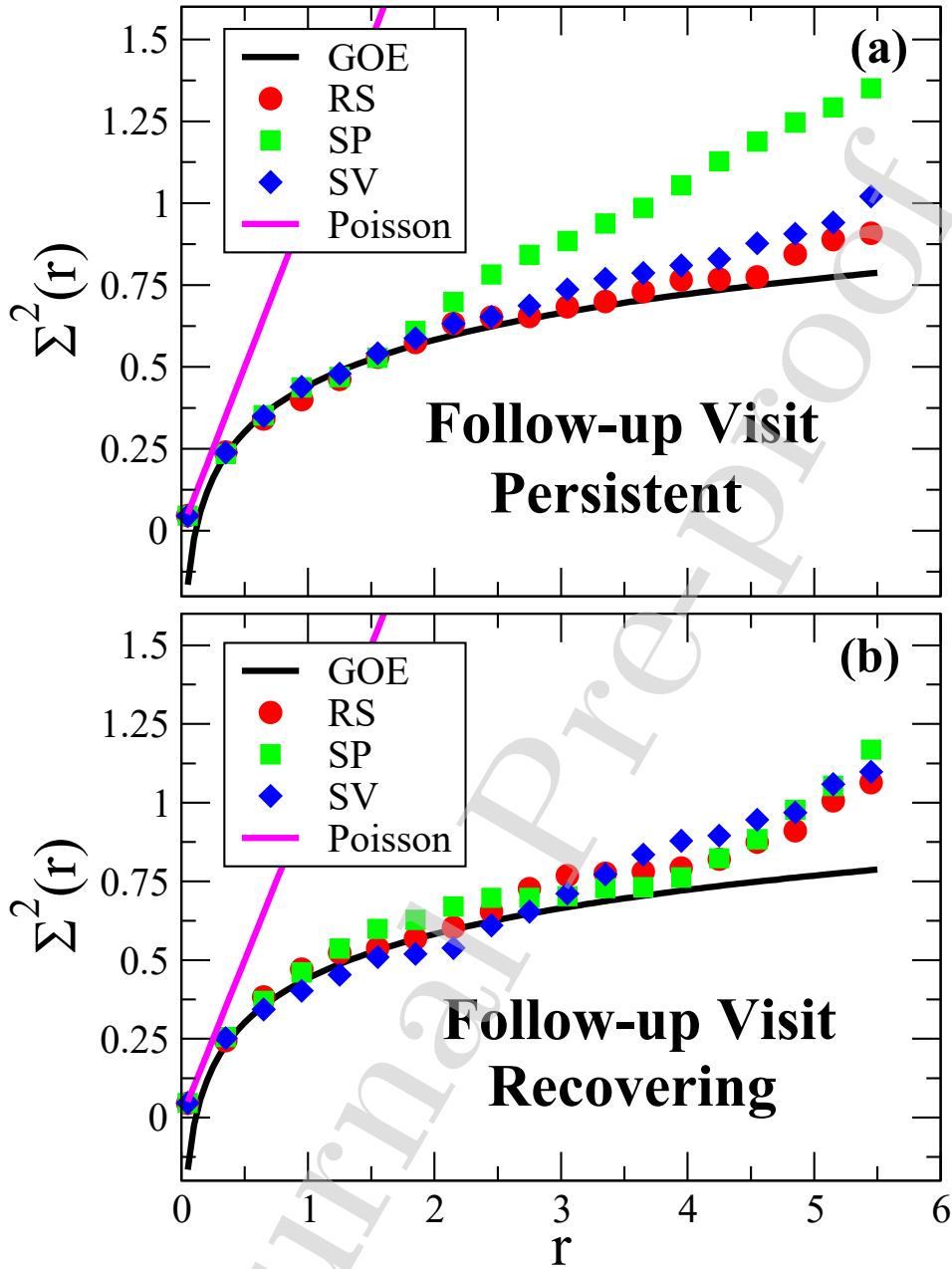


444 **Fig. 3: (a)** Normalized neighbor spacing ( $s$ ) vs probability density  $p(s)$  for resting state (red  
 445 circles), spontaneous pain (green squares), and standard visual (blue diamonds) scans for the  
 446 initial visit. Black line represents GOE prediction and magenta line represents Poisson  
 447 distribution; **(b)** Variance of the number of levels in intervals of length  $r$  shown as a function of  $r$   
 448 for resting state (red circles), spontaneous pain (green squares), and standard visual (blue  
 449 diamonds) for the initial visit. Black line represents GOE prediction and magenta line represents  
 450 Poisson distribution.  
 451



452  
 453 **Fig. 4:** Normalized neighbor spacing ( $s$ ) vs probability density  $p(s)$  for resting state (red circles),  
 454 spontaneous pain (green squares), and standard visual (blue diamonds) scans for (a) Persistent,  
 455 and (b) Recovering groups in the follow-up visit. Black line represents GOE prediction and  
 456 magenta line represents Poisson distribution.

457  
 458  
 459  
 460



461  
 462  
 463  
 464  
 465  
 466  
 467  
 468  
 469  
 470

**Fig. 5:** Variance of the number of levels in intervals of length  $r$  shown as a function of  $r$  for resting state (red circles), spontaneous pain (green squares), and standard visual (blue diamonds) for (a) Persistent, and (b) Recovering groups in the follow-up visit. For both visits, black line represents GOE prediction and magenta line represents Poisson distribution.

**471 Availability of data and materials**

472  
473 Data used in the preparation of this work were obtained from the OpenPain Project (OPP) database  
474 ([www.openpain.org](http://www.openpain.org)). The OPP project (Principal Investigator: A. Vania Apkarian, Ph.D. at  
475 Northwestern University) is supported by the National Institute of Neurological Disorders and  
476 Stroke (NINDS) and National Institute of Drug Abuse (NIDA).

477  
478 The preprocessing codes and the behavioral data (including MPQVAS data) used for the present  
479 work could be obtained by request from the authors.

480  
481 **Acknowledgements:** GSM would like to thank Karl-Peter Marzlin for useful discussions and  
482 suggestions. We thank ACENET and Compute Canada for computational resources.

483  
484 **Funding:** This research did not receive any specific grant from funding agencies in the public,  
485 commercial, or not-for-profit sectors.

486  
487 **Conflict of Interest:** The authors declare no conflict of interest

**488**  
**489 References**

- 490  
491 [1] J.D. Loeser, *Relieving pain in America*, National Academies Press, Washington, D.C.,  
492 2012. doi:10.1097/AJP.0b013e318230f6c1.
- 493 [2] J.A. Hashmi, A.T. Baria, M.N. Baliki, L. Huang, T.J. Schnitzer, V.A. Apkarian, Brain  
494 networks predicting placebo analgesia in a clinical trial for chronic back pain, *Pain*. 153  
495 (2012) 2393–2402. doi:10.1016/j.pain.2012.08.008.
- 496 [3] J.A. Hashmi, M.N. Baliki, L. Huang, A.T. Baria, S. Torbey, K.M. Hermann, T.J.  
497 Schnitzer, A.V. Apkarian, : A Vania Apkarian, Shape shifting pain: Chronification of  
498 back pain shifts brain representation from nociceptive to emotional circuits, *Brain*. 136  
499 (2013) 2751–2768. doi:10.1093/brain/awt211.
- 500 [4] H. Mano, G. Kotecha, K. Leibnitz, T. Matsubara, A. Nakae, N. Shenker, M. Shibata, V.  
501 Voon, W. Yoshida, M. Lee, T. Yanagida, M. Kawato, M.J. Rosa, B. Seymour,  
502 Classification and characterisation of brain network changes in chronic back pain: A  
503 multicenter study, *Wellcome Open Res.* 3 (2018) 19.  
504 doi:10.12688/wellcomeopenres.14069.1.
- 505 [5] M.N. Baliki, D.R. Chialvo, P.Y. Geha, R.M. Levy, R.N. Harden, T.B. Parrish, A. V.  
506 Apkarian, Chronic Pain and the Emotional Brain: Specific Brain Activity Associated with  
507 Spontaneous Fluctuations of Intensity of Chronic Back Pain, *J. Neurosci.* 26 (2006)  
508 12165–12173. doi:10.1523/JNEUROSCI.3576-06.2006.
- 509 [6] S. Ryali, T. Chen, K. Supekar, V. Menon, Estimation of functional connectivity in fMRI  
510 data using stability selection-based sparse partial correlation with elastic net penalty,  
511 *Neuroimage*. 59 (2012) 3852–3861. doi:10.1016/j.neuroimage.2011.11.054.
- 512 [7] T.O. Laumann, A.Z. Snyder, A. Mitra, E.M. Gordon, C. Gratton, B. Adeyemo, A.W.  
513 Gilmore, S.M. Nelson, J.J. Berg, D.J. Greene, J.E. McCarthy, E. Tagliazucchi, H. Laufs,  
514 B.L. Schlaggar, N.U.F. Dosenbach, S.E. Petersen, On the Stability of BOLD fMRI  
515 Correlations., *Cereb. Cortex*. 27 (2017) 4719–4732. doi:10.1093/cercor/bhw265.
- 516 [8] D.A. Seminowicz, T.H. Wideman, L. Naso, Z. Hatami-Khoroushahi, S. Fallatah, M.A.



- 517 Ware, P. Jarzem, M.C. Bushnell, Y. Shir, J.A. Ouellet, L.S. Stone, Effective Treatment of  
518 Chronic Low Back Pain in Humans Reverses Abnormal Brain Anatomy and Function, *J.*  
519 *Neurosci.* 31 (2011) 7540–7550. doi:10.1523/JNEUROSCI.5280-10.2011.
- 520 [9] M.N. Baliki, P.Y. Geha, A. V. Apkarian, D.R. Chialvo, Beyond Feeling: Chronic Pain  
521 Hurts the Brain, Disrupting the Default-Mode Network Dynamics, *J. Neurosci.* 28 (2008)  
522 1398–1403. doi:10.1523/JNEUROSCI.4123-07.2008.
- 523 [10] M.N. Baliki, T.J. Schnitzer, W.R. Bauer, A.V. Apkarian, Brain Morphological Signatures  
524 for Chronic Pain, *PLoS One.* 6 (2011) e26010. doi:10.1371/journal.pone.0026010.
- 525 [11] E. Tagliazucchi, P. Balenzuela, D. Fraiman, D.R. Chialvo, Brain resting state is disrupted  
526 in chronic back pain patients, *Neurosci. Lett.* 485 (2010) 26–31.  
527 doi:10.1016/j.neulet.2010.08.053.
- 528 [12] R. Yu, R.L. Gollub, R. Spaeth, V. Napadow, A. Wasan, J. Kong, Disrupted functional  
529 connectivity of the periaqueductal gray in chronic low back pain., *NeuroImage. Clin.* 6  
530 (2014) 100–8. doi:10.1016/j.nicl.2014.08.019.
- 531 [13] G. Tononi, G.M. Edelman, O. Sporns, Complexity and coherency: integrating information  
532 in the brain., *Trends Cogn. Sci.* 2 (1998) 474–84.  
533 <http://www.ncbi.nlm.nih.gov/pubmed/21227298> (accessed October 19, 2018).
- 534 [14] F. Crick, C. Koch, A framework for consciousness, *Nat. Neurosci.* 6 (2003) 119–126.  
535 doi:10.1038/nn0203-119.
- 536 [15] D.J. Watts, S.H. Strogatz, Collective dynamics of ‘small-world’ networks, *Nature.* 393  
537 (1998) 440–442. doi:10.1038/30918.
- 538 [16] T.A. Brody, J. Flores, J.B. French, P.A. Mello, A. Pandey, S.S.M. Wong, Random-matrix  
539 physics: spectrum and strength fluctuations, *Rev. Mod. Phys.* 53 (1981) 385–479.  
540 doi:10.1103/RevModPhys.53.385.
- 541 [17] T. Guhr, A. Müller-Groeling, H.A. Weidenmüller, Random-matrix theories in quantum  
542 physics: common concepts, 1998. [https://ac.els-cdn.com/S0370157397000884/1-s2.0-](https://ac.els-cdn.com/S0370157397000884/1-s2.0-S0370157397000884-main.pdf?_tid=c74e85ab-91ea-4241-9c2c-bcbde9897d72&acdnat=1548187209_7eb224f592156ade5d7e052f74d2774b)  
543 [S0370157397000884-main.pdf?\\_tid=c74e85ab-91ea-4241-9c2c-](https://ac.els-cdn.com/S0370157397000884-main.pdf?_tid=c74e85ab-91ea-4241-9c2c-bcbde9897d72&acdnat=1548187209_7eb224f592156ade5d7e052f74d2774b)  
544 [bcbde9897d72&acdnat=1548187209\\_7eb224f592156ade5d7e052f74d2774b](https://ac.els-cdn.com/S0370157397000884-main.pdf?_tid=c74e85ab-91ea-4241-9c2c-bcbde9897d72&acdnat=1548187209_7eb224f592156ade5d7e052f74d2774b) (accessed  
545 January 22, 2019).
- 546 [18] C.W.J. Beenakker, Random-matrix theory of quantum transport, *Rev. Mod. Phys.* 69  
547 (1997) 731–808. doi:10.1103/RevModPhys.69.731.
- 548 [19] O. Bohigas, M.J. Giannoni, C. Schmit, Characterization of Chaotic Quantum Spectra and  
549 Universality of Level Fluctuation Laws, *Phys. Rev. Lett.* 52 (1984) 1–4.  
550 doi:10.1103/PhysRevLett.52.1.
- 551 [20] T.H. Seligman, J.J.M. Verbaarschot, M.R. Zirnbauer, Quantum Spectra and Transition  
552 from Regular to Chaotic Classical Motion, *Phys. Rev. Lett.* 53 (1984) 215–217.  
553 doi:10.1103/PhysRevLett.53.215.
- 554 [21] O. Bohigas, R.U. Haq, A. Pandey, Higher-Order Correlations in Spectra of Complex  
555 Systems, *Phys. Rev. Lett.* 54 (1985) 1645–1648. doi:10.1103/PhysRevLett.54.1645.
- 556 [22] D. Wintgen, H. Marxer, Level statistics of a quantized cantori system, *Phys. Rev. Lett.* 60  
557 (1988) 971–974. doi:10.1103/PhysRevLett.60.971.
- 558 [23] A. Pandey, S. Ghosh, Skew-Orthogonal Polynomials and Universality of Energy-Level  
559 Correlations, *Phys. Rev. Lett.* 87 (2001) 024102. doi:10.1103/PhysRevLett.87.024102.
- 560 [24] M.L. Mehta, *Random Matrices*, Volume 142, Third Edition, 2004.
- 561 [25] M.S. Santhanam, P.K. Patra, Statistics of atmospheric correlations, *Phys. Rev. E.* 64  
562 (2001) 016102. doi:10.1103/PhysRevE.64.016102.

- 563 [26] V. Plerou, P. Gopikrishnan, B. Rosenow, L.A.N. Amaral, T. Guhr, H.E. Stanley, L.A.  
564 Nunes Amaral, T. Guhr, H. Eugene Stanley, Random matrix approach to cross  
565 correlations in financial data, *Phys. Rev. E.* 65 (2002) 066126.  
566 doi:10.1103/PhysRevE.65.066126.
- 567 [27] J.N. Bandyopadhyay, S. Jalan, Universality in complex networks: Random matrix  
568 analysis, *Phys. Rev. E - Stat. Nonlinear, Soft Matter Phys.* 76 (2007).  
569 doi:10.1103/PhysRevE.76.026109.
- 570 [28] S. Jalan, C. Sarkar, A. Madhusudanan, S.K. Dwivedi, Uncovering randomness and  
571 success in society, *PLoS One.* 9 (2014). doi:10.1371/journal.pone.0088249.
- 572 [29] S. Sastry, N. Deo, S. Franz, Spectral statistics of instantaneous normal modes in liquids  
573 and random matrices, *Phys. Rev. E.* 64 (2001) 016305. doi:10.1103/PhysRevE.64.016305.
- 574 [30] G.S. Matharoo, M.S.G. Razul, P.H. Poole, Spectral statistics of the quenched normal  
575 modes of a network-forming molecular liquid, *J. Chem. Phys.* 130 (2009) 124512.  
576 doi:10.1063/1.3099605.
- 577 [31] S.K. Sarkar, G.S. Matharoo, A. Pandey, Universality in the Vibrational Spectra of Single-  
578 Component Amorphous Clusters, *Phys. Rev. Lett.* 92 (2004) 215503.  
579 doi:10.1103/PhysRevLett.92.215503.
- 580 [32] G.S. Matharoo, S.K. Sarkar, A. Pandey, Vibrational spectra of amorphous clusters:  
581 Universal aspects, *Phys. Rev. B.* 72 (2005) 075401. doi:10.1103/PhysRevB.72.075401.
- 582 [33] G.S. Matharoo, Universality in the Vibrational Spectra of Amorphous Systems, 2005.  
583 doi:10.1088/0953-8984/21/5/055402.
- 584 [34] G.S. Matharoo, Universality in the vibrational spectra of weakly-disordered two-  
585 dimensional clusters, *J. Phys. Condens. Matter.* 21 (2009) 055402. doi:10.1088/0953-  
586 8984/21/5/055402.
- 587 [35] I. Osorio, Y.-C. Lai, A phase-synchronization and random-matrix based approach to  
588 multichannel time-series analysis with application to epilepsy, *Chaos An Interdiscip. J.*  
589 *Nonlinear Sci.* 21 (2011) 033108. doi:10.1063/1.3615642.
- 590 [36] P. Bhadola, N. Deo, Targeting functional motifs of a protein family, *Phys. Rev. E.* 94  
591 (2016) 1–13. doi:10.1103/PhysRevE.94.042409.
- 592 [37] A. Agrawal, C. Sarkar, S.K. Dwivedi, N. Dhasmana, S. Jalan, Quantifying randomness in  
593 protein–protein interaction networks of different species: A random matrix approach,  
594 *Phys. A Stat. Mech. Its Appl.* 404 (2014) 359–367. doi:10.1016/J.PHYSA.2013.12.005.
- 595 [38] A. Rai, A.V. Menon, S. Jalan, Randomness and preserved patterns in cancer network, *Sci.*  
596 *Rep.* 4 (2014). doi:10.1038/srep06368.
- 597 [39] P. Šeba, Random matrix analysis of human eeg data, *Phys. Rev. Lett.* 91 (2003) 1–4.  
598 doi:10.1103/PhysRevLett.91.198104.
- 599 [40] R. Wang, Z.-Z. Zhang, J. Ma, Y. Yang, P. Lin, Y. Wu, Spectral properties of the temporal  
600 evolution of brain network structure, *Chaos An Interdiscip. J. Nonlinear Sci.* 25 (2015)  
601 123112. doi:10.1063/1.4937451.
- 602 [41] R. Wang, L. Wang, Y. Yang, J. Li, Y. Wu, P. Lin, Random matrix theory for analyzing  
603 the brain functional network in attention deficit hyperactivity disorder, *Phys. Rev. E.* 94  
604 (2016) 20–23. doi:10.1103/PhysRevE.94.052411.
- 605 [42] A.V. Apkarian, B.R. Krauss, B.E. Fredrickson, N.M. Szeverenyi, Imaging the pain of low  
606 back pain: functional magnetic resonance imaging in combination with monitoring  
607 subjective pain perception allows the study of clinical pain states, *Neurosci. Lett.* 299  
608 (2001) 57–60. doi:10.1016/S0304-3940(01)01504-X.

- 609 [43] B.B. Biswal, M. Mennes, X.-N. Zuo, S. Gohel, C. Kelly, S.M. Smith, C.F. Beckmann, J.S.  
610 Adelstein, R.L. Buckner, S. Colcombe, A.-M. Dogonowski, M. Ernst, D. Fair, M.  
611 Hampson, M.J. Hoptman, J.S. Hyde, V.J. Kiviniemi, R. Kotter, S.-J. Li, C.-P. Lin, M.J.  
612 Lowe, C. Mackay, D.J. Madden, K.H. Madsen, D.S. Margulies, H.S. Mayberg, K.  
613 McMahon, C.S. Monk, S.H. Mostofsky, B.J. Nagel, J.J. Pekar, S.J. Peltier, S.E. Petersen,  
614 V. Riedl, S.A.R.B. Rombouts, B. Rypma, B.L. Schlaggar, S. Schmidt, R.D. Seidler, G.J.  
615 Siegle, C. Sorg, G.-J. Teng, J. Veijola, A. Villringer, M. Walter, L. Wang, X.-C. Weng, S.  
616 Whitfield-Gabrieli, P. Williamson, C. Windischberger, Y.-F. Zang, H.-Y. Zhang, F.X.  
617 Castellanos, M.P. Milham, Toward discovery science of human brain function, *Proc. Natl.*  
618 *Acad. Sci.* 107 (2010) 4734–4739. doi:10.1073/pnas.0911855107.
- 619 [44] J.A. Hashmi, M.L. Loggia, S. Khan, L. Gao, J. Kim, V. Napadow, E.N. Brown, O. Akeju,  
620 Dexmedetomidine Disrupts the Local and Global Efficiencies of Large-scale Brain  
621 Networks, *Anesthesiology*. 126 (2017) 419–430. doi:10.1097/ALN.0000000000001509.
- 622 [45] J.A. Hashmi, J. Kong, R. Spaeth, S. Khan, T.J. Kaptchuk, R.L. Gollub, Functional  
623 Network Architecture Predicts Psychologically Mediated Analgesia Related to Treatment  
624 in Chronic Knee Pain Patients, *J. Neurosci.* 34 (2014) 3924–3936.  
625 doi:10.1523/JNEUROSCI.3155-13.2014.
- 626 [46] C. Kelly, R. Toro, A. Di Martino, C.L. Cox, P. Bellec, F.X. Castellanos, M.P. Milham, A  
627 convergent functional architecture of the insula emerges across imaging modalities,  
628 *Neuroimage*. 61 (2012) 1129–1142. doi:10.1016/j.neuroimage.2012.03.021.
- 629 [47] M. Rubinov, O. Sporns, Complex network measures of brain connectivity: Uses and  
630 interpretations, *Neuroimage*. 52 (2010) 1059–1069.  
631 doi:10.1016/j.neuroimage.2009.10.003.
- 632 [48] V.M. Eguíluz, D.R. Chialvo, G.A. Cecchi, M. Baliki, A.V. Apkarian, Scale-free brain  
633 functional networks, *Phys. Rev. Lett.* 94 (2005) 1–4. doi:10.1103/PhysRevLett.94.018102.
- 634 [49] D. Fraiman, P. Balenzuela, J. Foss, D.R. Chialvo, Ising-like dynamics in large-scale  
635 functional brain networks, *Phys. Rev. E - Stat. Nonlinear, Soft Matter Phys.* 79 (2009) 1–  
636 10. doi:10.1103/PhysRevE.79.061922.
- 637 [50] T. Wirtz, M. Kieburg, T. Guhr, Limiting statistics of the largest and smallest eigenvalues  
638 in the correlated Wishart model, *EPL (Europhysics Lett.)* 109 (2015) 20005.  
639 doi:10.1209/0295-5075/109/20005.
- 640 [51] N. Masuda, S. Kojaku, Y. Sano, Configuration model for correlation matrices preserving  
641 the node strength, *Phys. Rev. E*. 98 (2018) 1–18. doi:10.1103/PhysRevE.98.012312.
- 642 [52] A.V. Apkarian, Y. Sosa, S. Sonty, R.M. Levy, R.N. Harden, T.B. Parrish, D.R. Gitelman,  
643 Chronic back pain is associated with decreased prefrontal and thalamic gray matter  
644 density., *J. Neurosci.* 24 (2004) 10410–5. doi:10.1523/JNEUROSCI.2541-04.2004.
- 645 [53] F. Cauda, T. Costa, M. Diano, K. Sacco, S. Duca, G. Geminiani, D.M.E. Torta, Massive  
646 Modulation of Brain Areas After Mechanical Pain Stimulation: A Time-Resolved fMRI  
647 Study, *Cereb. Cortex*. 24 (2014) 2991–3005. doi:10.1093/cercor/bht153.
- 648 [54] D. Borsook, R. Edwards, I. Elman, L. Becerra, J. Levine, Pain and analgesia: the value of  
649 salience circuits., *Prog. Neurobiol.* 104 (2013) 93–105.  
650 doi:10.1016/j.pneurobio.2013.02.003.
- 651 [55] S. Geuter, E.A.R. Losin, M. Roy, L.Y. Atlas, L. Schmidt, A. Krishnan, L. Koban, T.D.  
652 Wager, M.A. Lindquist, Multiple brain networks mediating stimulus-pain relationships in  
653 humans, (n.d.). doi:10.1101/298927.
- 654

655 **Highlights:**

656

657 • **Brain networks impacted by back-pain are analyzed from random matrix theory**  
658 **perspective.**

659

660 • **The study demonstrates the effectiveness of random matrix theory in differentiating**  
661 **between resting state and two distinct task states within the same patient.**

662

663 • **Random matrix theory is effective in measuring systematic changes occurring in**  
664 **functional connectivity.**

665

666 • **This study offers new insights on how acute and chronic pain are processed in the**  
667 **brain at a network level.**

668

669

670

671 **Declaration of interests**

672

673 The authors declare that they have no known competing financial interests or personal  
674 relationships that could have appeared to influence the work reported in this paper.

675

676

677

678

679

680

681